

Semi-automatic retractable handrail utilizing opening/closing movement of sliding door supporting elderly people to walk independently

著者	Saitou Kinjiro, Noda Nao-Aki, Sano Yoshikazu, Takase Yasushi, Li Shuqiong, Tanaka Hiroyuki, Kubo Yoshitaka
journal or publication title	Journal of Accessibility and Design for All
volume	11
number	1
page range	1-20
year	2021-05-31
その他のタイトル	Semi-Automatic Retractable Handrail Utilizing Opening/Closing of Sliding Door Supporting Elderly People to Walk Independently
URL	http://hdl.handle.net/10228/00008287

doi: <https://doi.org/10.17411/jacces.v11i1.327>

SEMI-AUTOMATIC RETRACTABLE HANDRAIL UTILIZING OPENING/CLOSING MOVEMENT OF SLIDING DOOR SUPPORTING ELDERLY PEOPLE TO WALK INDEPENDENTLY

Kinjiro Saitou¹, Nao-Aki Noda^{2*}, Yoshikazu Sano³, Yasushi Takase⁴,
Shuqiong Li⁵, Hiroyuki Tanaka⁶, & Yoshitaka Kubo⁷

¹Yahata Rolling Mechanical Engineering Department, Engineering Division,
Mechanical Engineering Unit, NIPPON STEEL TEXENG. CO., LTD., Kitakyushu-shi,
Fukuoka, Japan

^{2,3,4,5,6}Department of Mechanical Engineering, Kyushu Institute of Technology,
Kitakyushu-Shi, Fukuoka, Japan

⁷Architecture Engineering Department, Development Division, Kei Products Co.,
Ltd., Kitakyushu-shi, Fukuoka, Japan

¹ ORCID: 000-0001-7983-7070, ² ORCID: 0000-0002-6044-6974

¹ saitou613@jcom.zaq.ne.jp, ² noda.naoaki844@mail.kyutech.jp,

³ sano.yoshikazu029@mail.kyutech.jp, ⁴ takase.yasushi415@mail.kyutech.jp
⁵ 1558609579@qq.com, ⁶ hiro-hiro5123@jcom.home.ne.jp, ⁷ keipro21@iwk.bbiq.jp

*corresponding author

Received: 2021-02-02 | Accepted: 2021-03-31 | Published: 2021-05-31

Abstract: The purpose of this research is to install a handrail on the sliding doors used in hospitals and nursing facilities to support senior and people with disabilities to walk by themselves. The semi-automatic lifting equipment is utilized for the retractable handrail to make sure people in bad health are able to open the door using a weak force. To design the handrail for this purpose, the theoretical formula for opening force is derived. Then the simulation is performed with varying geometry conditions confirming the results are in good agreement with the experiment results. The opening force is designed to be less than the target value previously reported. The sliding door developed in this study is useful for elderly people walking by themselves safely.

Keywords: sliding door; handrail; opening force; simulation; people with disabilities.

Nomenclature

The following notations will be used in this paper.

$F_{Ax}(x_A)$: Opening force applied at point A in Figure 6. Target value
 $F_{Ax}(x_A) = 19.6$ N

$F_{Ay}(x_A)$: Reaction force applied to handrail at point A ($x_A, 0$) in y-direction in Figure 6

$(x_A, y_A) = (x_A, 0)$: Coordinates of supporting point A in Figure 5, x_A = Opening distance of sliding door

(x_{B0}, y_{B0}) : Coordinates of point B in Figure 5, Point B = Center of guide roller

(x_D, y_D) : Coordinates of point D in Figure 5, Point D = Center of arc portion of guide rail

Q : $Q = \mu_t P$, Running resistance (see Figure 6)

P : Reaction force to handrail from guide rail at point B in Figure 6

R : Rolling surface radius of guide rail stand in Figure 5
($R = 478$ mm, for prototype)

θ : Angle between retractable handrail and horizontal line (see Figure 5)

φ : Handrail angle between tangential direction of guiderail at B and handrail (see Figure 5)

ε : Guide rail angle between tangential direction of guiderail and vertical direction (see Figure 5)

- W : Weight of handrail including guide roller in Figure 6 ($W = 13.7$ N, for prototype steel handrail)
- M : Moment due to torsion spring in Figure 6 ($M = k(0.5\pi - \theta)$)
- k : Spring constant ($k = 2395$ N mm/rad)
- μ_t : Friction coefficient of bearing 0.03 + friction coefficient of rotating roller 0.05 in Figure 6 ($\mu_t = 0.03 + 0.005 = 0.035$) (Ando, 1968)
- a : $a = y_A - y_{B0}$, AB in y-direction in Figure 6 ($a = 22.6$ mm, for prototype)
- b : Horizontal difference, $b = x_A - x_{B0}$, between point A and point B in Figure 5 ($b = 910.3$ mm, for prototype)
- c : Distance from guide roller contact point to rail vertical point in Figure 5 ($c = 58.2$ mm, for prototype)
- r : Radius of guide roller B in Figure 5 ($r = 17.5$ mm for prototype)
- e : Distance in x-direction between center point of guide roller B and contact point of roller and rail in Figure 5
- l : Length of retractable handrail rod in Figure 5 ($l = 910.3$ mm for prototype)
- C : Contact point of roller in Figure 5
- E : End point of curved portion of guide rail in Figure 5
- F : Guide rail end in Figure 5

Introduction

Sliding doors have many advantages compared to hinged doors popularly used in the world. No space is necessary during the opening, people can feel a sense of freedom due to the door fitting inside the wall, and the smaller movement of the body is suitable for elderly people opening/closing. In Japan, therefore,

a lot of sliding doors are conventionally used as interior doors in private houses, hospitals, and welfare facilities. Figure 1 shows examples of sliding doors used in Japanese welfare facilities.

As shown in Figure 1, to support elderly people to walk independently, many residential buildings, nursing homes and hospitals have installed handrails along all over the corridor walls. However, if there is a sliding door in the middle of the corridor, a handrail cannot be installed on the sliding door surface because the sliding door cannot be opened and closed. Because of no handrail on the sliding door, it would be difficult for elderly people to go to the bathroom alone. It is, therefore, necessary to install handrails continuously without interruption for elderly people. When elderly and people with disabilities can walk by themselves, it is known that such decline prevention measures are useful for maintaining and restoring their walking function (Gault & Willems, 2013; Porter, Vandervoort, & Lexell, 1995; World Health Organization, 2007).

Figure 1. Examples of sliding doors used in Japanese welfare facilities.

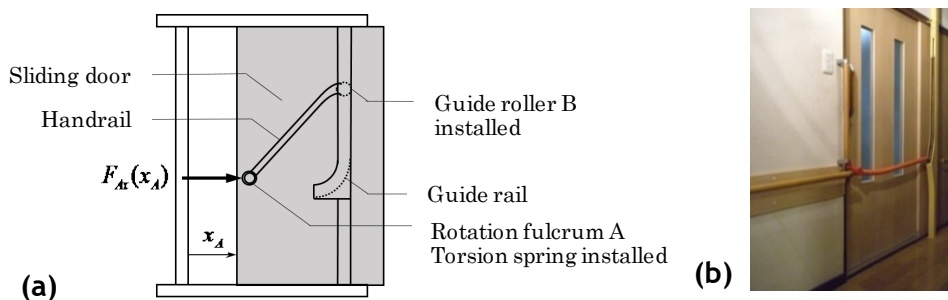


In addition, installing handrails over the entire length of the corridors eliminates risks of falling during walking and increases their motivation to walk (Arfken, Lach, Birge, & Miller, 1994; Chu et al., 1999; Cumming, Salkeld, Thomas, & Szonyi, 2000; Gunter, White, Hayes, & Snow, 2000; Howland et al., 1998; Kim, Yoshida, & Suzuki, 2001; Lachman et al., 1998). From this viewpoint, in this study, the final goal is to develop a retractable handrail fixed on the surface of the sliding door (Kubo, 2011; Kubo, 2017) to support elderly people walking by themselves. This product is useful for maintaining

and restoring the walking function of elderly people by providing a self-support environment, which can contribute to a healthy life expectancy. Dozens of studies on handrails are found including handrail shapes intended to prevent falling over on stairs and handrail position designs for a movement from a seated to a standing position (Chihara & Seo, 2014; Dusenberry, Simoson, DelloRusso, & Rao, 2009; Ishihara et al., 2002; Min, Kim, & Parnianpour, 2012). However, research and development of handrails that can be attached to the sliding doors along corridors have not been well conducted. Additionally, several conventional products on sliding doors are currently available, which have a risk of falling off or falling down and cannot be used without the possibility of fear.

Figure 2 illustrates the retractable handrail on the sliding door considered in this study. This paper deals with how to design the handrail device to enable the safe use of elderly and people with disabilities. Specifically, experiments and numerical simulations were performed to clarify the effect of the retractable rail geometry on the opening force to enhance the operability of the sliding door with the retractable handrail during the opening.

Figure 2. Illustration of sliding door with retractable handrail: (a) Opening state of sliding door; (b) Sliding door with handrail.

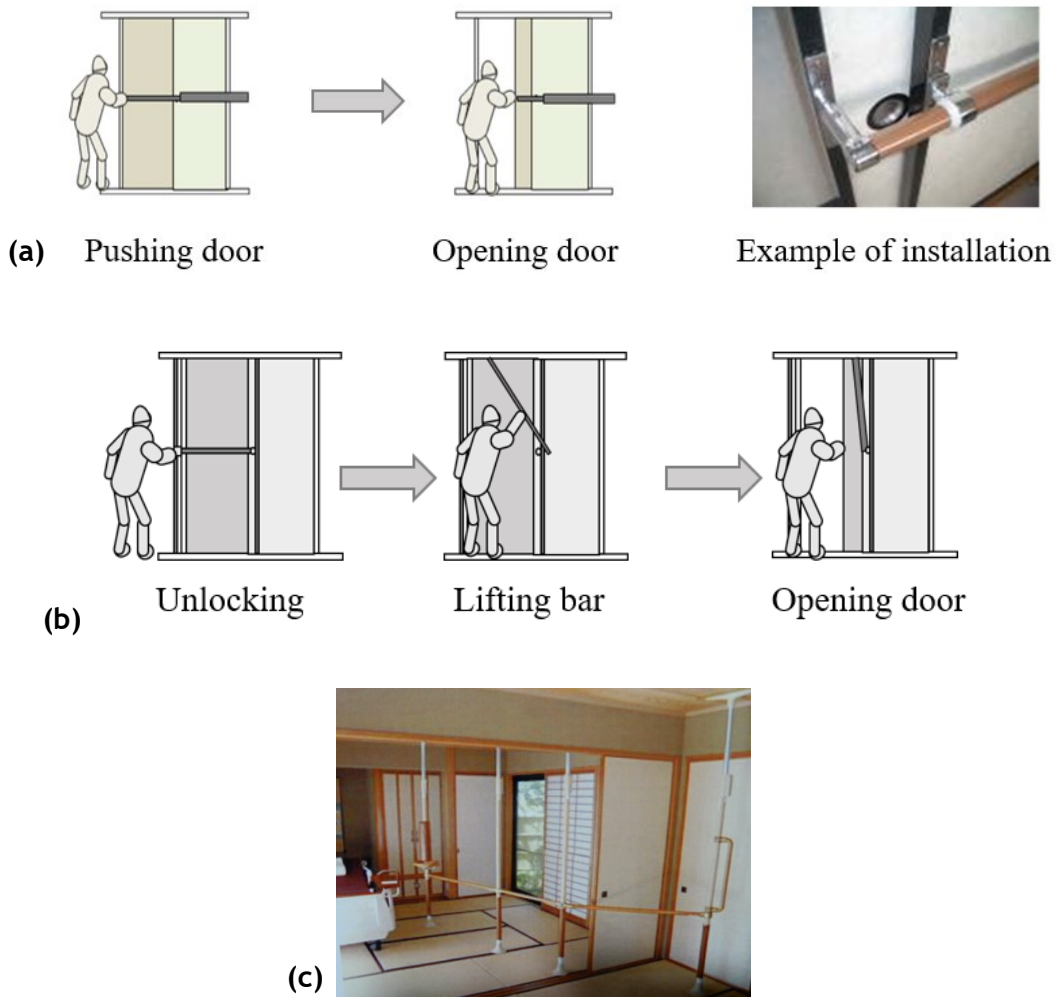


Conventional handrails on sliding doors and their problems

Figure 3 illustrates three kinds of conventional handrails closely related to the proposed retractable handrail in Figure 2. Figure 3(a) shows the telescopic type whose door may fall out from the threshold when the human weight is fully applied to the handrail (Itoh, 2007). Figure 3(b) shows the flip-up type

handrail (Mazroc Co., Ltd., 2019). Although the door may have enough strength, the flip-up operation of the handrail is difficult for elderly people. Figure 3(c) shows the stand type handrail (Kitamura, 2007), which can be installed easily in Japanese rooms. However, the structure is unstable because the vertical supporting force from tatami mats varies.

Figure 3. Conventional handrails closely related to Figure 1: (a) Telescopic type handrail attached on sliding door; (b) Flip-up type handrail attached on sliding door; (c) Stand type handrail installed in a Japanese room.

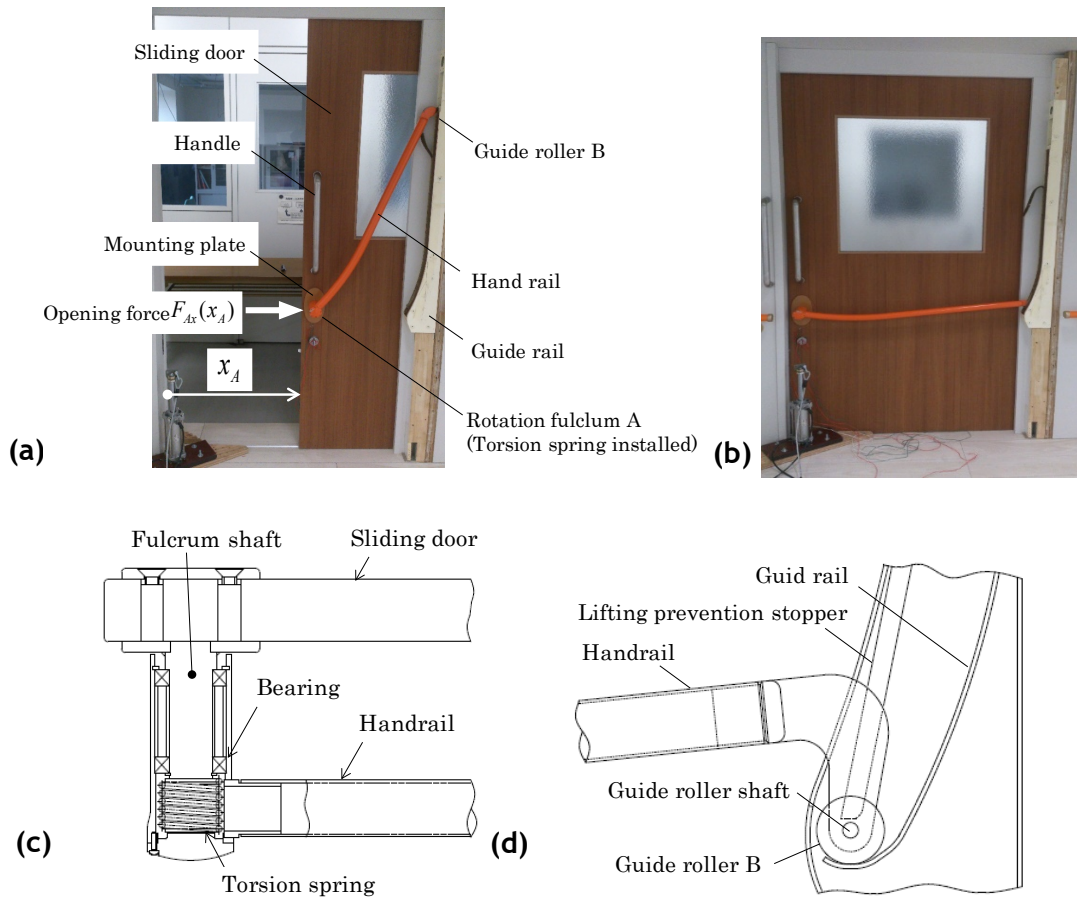


It is harsh for elderly people to stand with their trembling limbs, support their weight with one hand so as not to fall, operate the handrail with the remaining hand, and open the sliding door. In addition, there remains a concern about the door strength and safety. In this way, the conventional technology seems to have been designed mainly from the viewpoint of a healthy person.

Structure of sliding door with semi-automatic retractable handrail utilizing open/closing movement considered in this paper

Figure 4(a) shows the sliding door with the retractable handrail, which is composed of a sliding door, retractable handrail, rotation fulcrum, rotary roller of the retractable handrail and guide rail. Under the closed state of the sliding door, the retractable handrail becomes horizontal and functions as a handrail. Figure 4(b) shows the closed state of the sliding door. With the movement of opening the sliding door, the retractable handrail moves around the rotation fulcrum A, and the rotating roller B at the end of the handrail moves upward along the rolling surface inside the guide rail stand. In this way, the handrail is retracted by utilizing the opening movement. Due to the weight of the handrail, the sliding door can be closed automatically. Figure 4(d) shows the guide roller B and the guide rail. When the sliding door is closed, the retractable handrail moves downward along the rolling surface inside of the guide rail. Figure 4(c) shows the structure of the rotation fulcrum A with the built-in torsion spring. The torsion spring whose spring constant $k = 2395 \text{ N mm/rad}$ is equipped on the rotation fulcrum A (Sasuga, 2003). When the door is opened, the torsion spring supports the movement and the rotation of the handrail and reduces the opening force. In this way, the handrail is designed to be raised and lowered semi-automatically by utilizing the sliding door opening/closing movement. Therefore, even elderly people can easily open and close the door by their weak force, $2 \text{ kgf} = 19.6 \text{ N}$ or less (Tanaka et al., 2004). This sliding door can be opened with one hand, and it can be used by wheelchair users pushing and pulling the handrail with a small force. If the opening force of the sliding door can be design in a suitable way, it will be stable and easy for the users to use.

Figure 4. Retractable handrail on sliding door: (a) Opening state of sliding door; (b) Closed state of sliding door; (c) Structure of rotation fulcrum A; (d) Guide roller B and guide rail.



Simulation of sliding force

Equilibrium of handrail to obtain opening force

The numerical simulation is conducted to investigate the opening force. To simplify the simulation, the guide rail is assumed to consist of a curve and a straight line sections, as shown in Figure 7(b). Figure 5 illustrates the handrail model considered when the torsion spring M (in Figure 6) is not installed. Figure 6 shows the free body diagram of the handrail when the torsion spring is installed on the rotation support of the shaft. Equations (1) to (3) are derived from the equilibrium in Figure 6.

$$F_{Ax}(x_A) = Q \cos(\theta + \varphi) + P \sin(\theta + \varphi) \tag{1}$$

$$F_{Ay}(x_A) + P \cos(\theta + \varphi) = W + Q \sin(\theta + \varphi) \tag{2}$$

$$M + lP \cos \varphi = \frac{1}{2}lW \cos \theta + lQ \sin \varphi \tag{3}$$

From equations (1) to (3), the following expressions are obtained.

$$F_{Ax}(x_A) = \mu_t P \cos(\theta + \varphi) + P \sin(\theta + \varphi) \tag{4}$$

$$F_{Ay}(x_A) = W + \mu_t P \sin(\theta + \varphi) - P \cos(\theta + \varphi) \tag{5}$$

Figure 5. Schematic illustration of retractable handrail and guide rail.

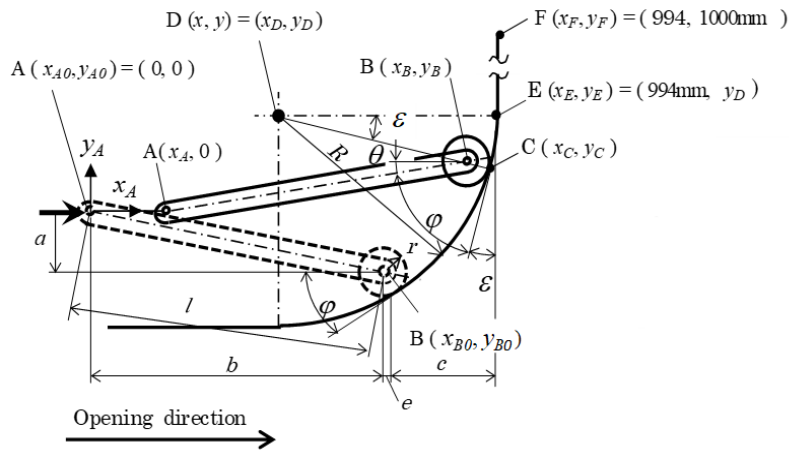
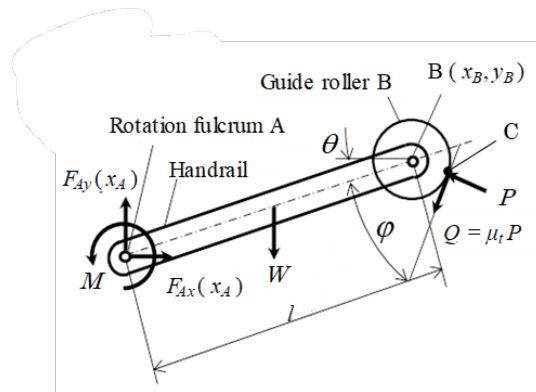


Figure 6. Equilibrium of external forces with torsion spring.



As shown in Figure 5, a Cartesian coordinate system (x, y) is used to describe the handrail position during the opening of the sliding door. When the sliding door is fully closed, the origin $(x, y) = (0, 0)$ is defined as the coordinates (x_A, y_A) of the rotation fulcrum A. Then, the door's position can be expressed by the position of point A as $x = x_A$. To describe the coordinates (x_{B0}, y_{B0}) at the

rotation fulcrum B, the angles θ and φ in Figure 5 will be used in relation to the coordinates of the centre point D at $(x, y) = (x_D, y_D)$ with the curvature radius R . The following equations can be used during the sliding door opening at $x = x_A$.

$$\theta = \tan^{-1} \frac{(y_B - y_{B0}) - a}{\sqrt{l^2 - ((y_B - y_{B0}) - a)^2}} \tag{6}$$

$$\varphi = 90^\circ - (\theta + \varepsilon) \tag{7}$$

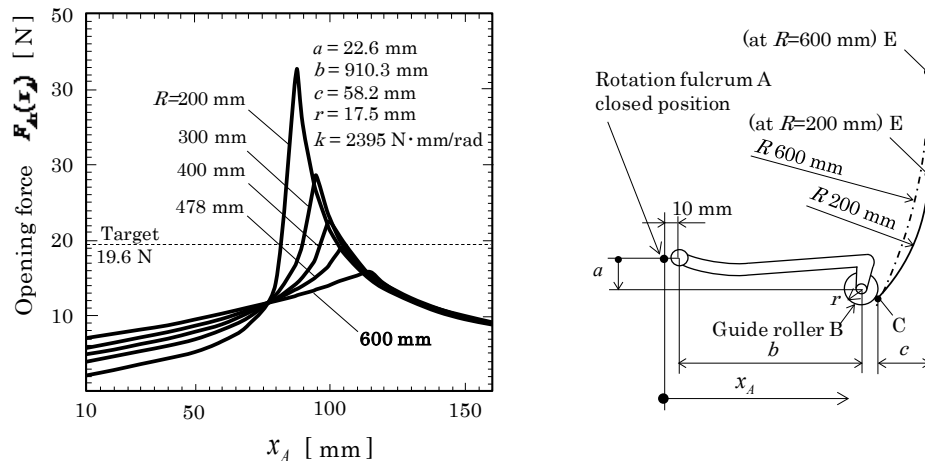
$$\varepsilon = \sin^{-1} \frac{y_D - (y_B - y_{B0})}{R - r} \tag{8}$$

As shown in equations (4) and (5), the opening force $F_{Ax}(x_A)$ includes equations (6) to (8). Note that the effect of the inertia force on the opening force $F_{Ax}(x_A)$ is small enough to be negligible.

Guiderail geometry and opening force

In this section, simple geometry of the guide rail is assumed. Then, the opening force is discussed. Figure 7(a) shows the simulation results of the opening force $F_{Ax}(x_A)$ obtained from equation (4) when $R = 200, 300, 400, 478,$ and 600 mm. Figure 7(b) illustrates the simulation model where the guide rail consists of a curve and a straight line sections.

Figure 7. Sliding force $F_{Ax}(x_A)$ in Figure 5 obtained from equation (4) by varying R : (a) Simulation value; (b) Simulation model.



In this modelling, the opening force is obtained when $x \gg 10$ mm since the guide rail geometry $0 \leq x \leq 10$ mm will be considered later. When the door is

at $x = 10$ mm, the guide roller B starts contacting the point C at the end of the circular arc in Figure 7(b). As shown in Figure 7(a), the opening force $F_{Ax}(x_A)$ increases gradually while the distance x_A is increasing and takes the maximum value in the vicinity of $x_A = 79$ to 105 mm, then decreases gradually. In Figure 7(a), the maximum opening force increases with decreasing R.

Discussion on maximum opening force

As shown in Figure 7(a), the opening force takes the maximum value at a certain distance around $x_A = 79$ to 105 mm. In this section, the distance x_A showing the maximum opening force is discussed. First, let us focus on the angle φ in Figure 5 between the handrail bar direction of the line AB and the tangential direction of the guide rail. Figure 8 illustrates three models having a different angle φ . When the angle $\varphi = 90^\circ$ in Figure 8(a), the force F_A acting perpendicularly to the guide rail cannot raise the point B in the upward direction. Instead, when $\varphi < 90^\circ$ as shown in Figure 8(b), the roller can be raised. When the angle φ is smaller as shown in Figure 8(c), the roller can be moved by a smaller force. Thus, when the angle φ approaches 90° , the opening force becomes greater.

Figure 8. Schematic illustration $F_{Ax}(x_A)$ depending on φ : (a) $\varphi = 90^\circ$; (b) $\varphi = \text{Middle} < 90^\circ$; $\varphi = \text{Small} \ll 90^\circ$.

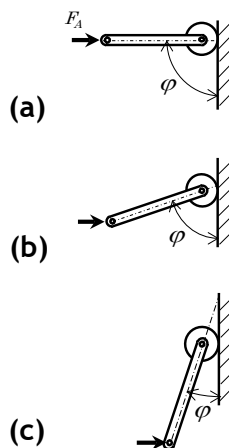
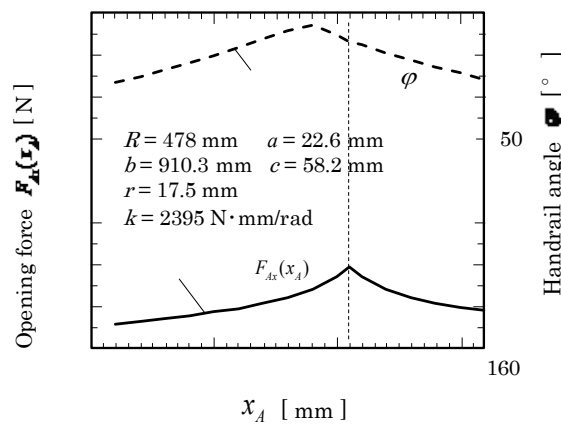


Figure 9 compares the sliding force $F_{Ax}(x_A)$ and the angle $\varphi(x_A)$ with respect to the opening distance x_A . The angle φ increases while the distance x_A is increasing and takes a peak value around the point E in Figure 5, then decreases. A similar behaviour can be seen for the sliding force $F_{Ax}(x_A)$. The peak value position of φ is slightly different from the peak value position of

$F_{Ax}(x_A)$ because the roller diameter affects the results. The maximum opening force $F_{Ax}(x_A)$ appearing in a convex form can be explained with the angle φ variation. The maximum opening force appears when the point B locates at the circular arc end point E in Figure 5 where the straight portion starts. Tanaka et al. (Tanaka et al., 2004) reported that the opening force of 20 N or less is suitable for elderly people. Therefore, in this study, based on the target opening force $F_{Ax}(x_A) = 2 \text{ kgf} = 19.6 \text{ N}$, the radius of curvature of the prototype guide rail is designed as $R = 478 \text{ mm}$.

Figure 9. Opening force $F_{Ax}(x_A)$ closely related to angle $\varphi(x_A)$.



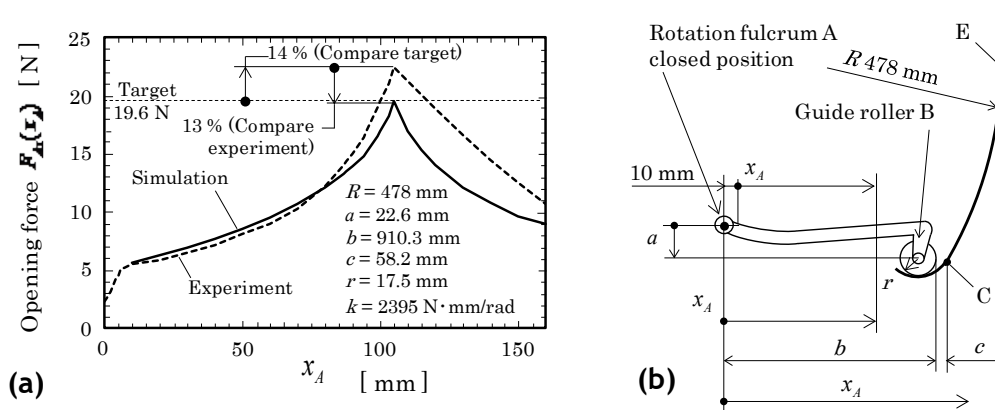
Prototype handrail geometry and opening force

Opening force of prototype sliding door

Figure 10(a) compares the analytical and experimental results of the opening force of the prototype handrail shown in Figure 10(b), whose $R = 478 \text{ mm}$. The experimental value is obtained using a spring scale in the range $0 \leq x_A \leq 160 \text{ mm}$, which is from the fully closed position to $x_A = 160 \text{ mm}$. The experimental opening force $F_{Ax}(x_A)$ increases sharply from $F_{Ax}(x_A) = 2.3$ to 5 N because the radius R is small (17.5 mm) at the lower end of the guide-rail, as shown in Figure 11(b). To start opening the door, 2.3 N is necessary. After that, both of the opening forces $F_{Ax}(x_A)$ analytically and experimentally obtained gradually increase and reach the maximum at the point S, then decreases. The analytical maximum value equation (4) $F_{Ax\text{max}} = 19.5 \text{ N}$ and the experimental maximum value $F_{Ax\text{max}}^{\text{Exp}} = 22.4 \text{ N}$ coincide with each other

within 13%. The difference is mainly caused by the guide rail fabrication and assembly errors. Equation (4) does not include the inertia force effect, but the error can be estimated within several percentage points.

Figure 10. Opening force $F_{AX}(x_A)$ of prototype sliding door: (a) Sliding force $F_{AX}(x_A)$ value; (b) Handrail model.



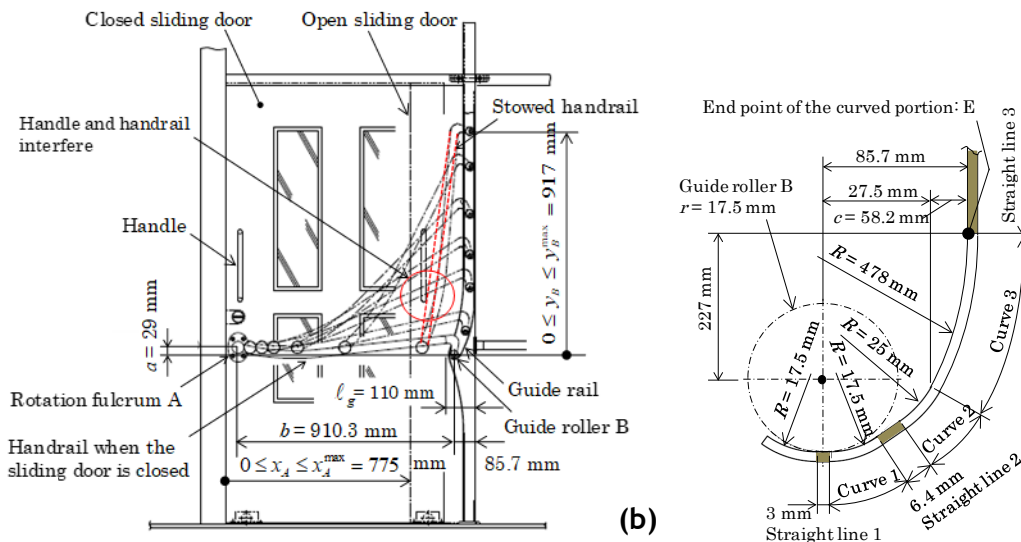
Although the simulation result when $R = 478$ mm in Figure 10(a) satisfies the target value $F_{Amax} \leq 19.6$ N, the experimental result $F_{Amax}^{Exp} = 22.4$ N is slightly greater than the target value by 2.8 N (14%). This difference of 2.8 N can be eliminated by adjusting the torsion spring attached to the rotation fulcrum A. It is concluded that the target opening force can be realized without changing the design specifications.

Details of prototype guide rail geometry

Figure 11(a) illustrates the movement of the retractable handrail. The feature is that the handrail on the sliding door in the horizontal state can be retracted vertically by the rotation around the rotation fulcrum A utilizing the movement of the sliding door opening. In addition to the small opening force 19.6 N shown in Figure 7(a), enough space is also required during the opening for wheelchairs to go through. Therefore, the dimension for storage shown as the notation l_g in Figure 11(a) should be designed as small as possible so that the retracted handrail as well as the guide-rail does not interfere with daily life during the opening. The following design specifications are set to satisfy those requirements. First, in Figure 11(a), the sliding door opening distance is set as $x_A^{max} = 775$ mm based on the wheelchair width of 700 mm. The horizontal dimension of the storage space l_g in Figure 11(a) is set as $l_g =$

110 mm to increase the opening distance. The relative positions between the rotation fulcrum A and the guide roller B are determined to realize the smooth movement of the handrail when the guide rail geometry is determined. In addition, as shown in Figure 11(a), the handrail is gently bent to avoid interference between the handle and the handrail when the sliding door is fully opened (see the red circle in Figure 11(a)).

Figure 11. Prototype retractable handrail trajectory and guide rail details: (a) Outline of sliding door device; (b) Detail of guide rail.



Next, the detailed geometry of the prototype guide rail will be explained. The smooth handrail movement totally depends on the guide rail. Figure 11(b) illustrates the guide rail geometry of the prototype determined after several trials. The guide rail geometry consists of three straight line and three circular arc sections. The straight line 1 and the circular arc 1 may allow the door's installation position error to close the door completely. The circular arc 2 and the straight line 2 are set to produce the initial opening force $F_{Ax}(x_A) = 5 \text{ N}$ in Figure 10(a). This is because a small initial opening force $F_{Ax}(x_A) < 5 \text{ N}$ is dangerous for elderly people. As shown in Figure 10(a), the opening force suddenly increases from $F_{Ax}(x_A) = 0$ at $x_A = 0$ to $F_{Ax}(x_A) \approx 5 \text{ N}$ at $x_A \approx 5 \text{ mm}$. The circular arc 3 with $R = 478 \text{ mm}$ is set to obtain the maximum opening force within 19.6 N. In this way, the prototype guide rail is suitable for opening the sliding door. It was also confirmed that the door is closed automatically due to the weight of the handrail. It should be noted that the closing speed

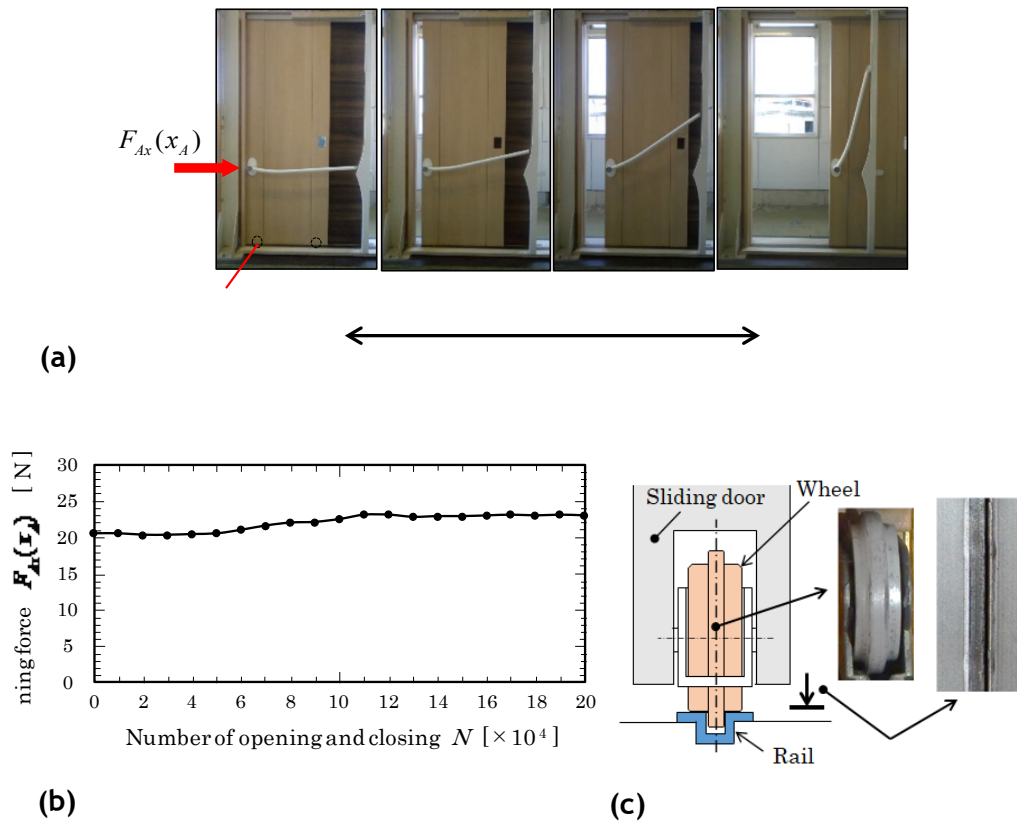
becomes slower at the end of the closing due to the smaller radiuses of the circular arcs 1 and 2.

Repeated opening/closing test for sliding door

Figure 12(a) illustrates a repeated opening/closing test condition for the sliding door. The second prototype equivalent to the first one, which was used for the measurement of the opening force $F_{Ax}(x_A)$, was used for this test. In this experiment, the door is opened and closed manually until the number of cycles reaches 200,000. The following procedure is repeated; grabbing the handrail handle, opening the sliding door until the position where the handrail is fully raised, and then fully closing the sliding door. The average speed is 12.5 cycles/min with a 775 mm sliding stroke. The opening force was measured with a spring meter every 10,000 cycles. When the door is opened, the maximum value was visually read. Figure 12(b) is the plot of the measured opening force values in the repeated opening/closing test. The opening force $F_{Ax}(x_A)$ gradually increases from 20.5 N at the beginning of the test, reaches the maximum value of 23.1 N at 110,000 times, then becomes almost constant until 200,000 times. The amount of increase in opening force is about 10%. This is because wear occurs on resin wheels supporting the door and on the rail surface due to the repeated opening/closing operations. The wear increases running resistance. After the test, the wear marks were found on the wheels and rail surface though they were new at the beginning of use.

Figure 12(c) shows the wear condition of the rail and wheel surfaces after the test. The main cause of this wear is considered to be jammed minute particles including dust as well as the rollers becoming overheated by the frequent and repeated operation of the sliding door. In the experimental condition of this case, the opening/closing speed of the sliding door is the same as that in normal use though the number of operation is high. This level of the change in the opening force is acceptable in function. The above-mentioned experiment confirms that the sliding door is capable of withstanding 200,000 times of repeated opening/closing use at the maximum without significant change.

Figure 12. Repeated opening/closing test for sliding door: (a) Repeated opening/closing test for sliding door; (b) Opening force vs number of cycles; (c) Rail and wheel wear.



Conclusions

In this study, to support the senior and people with disabilities to walk independently, a semi-automatic retractable handrail was developed utilizing opening/closing movement of the sliding door. The sliding door with the retractable handrail can be installed in hospitals and nursing facilities. A theoretical formula was derived from the equilibrium of the handrail to reduce the opening force. The conclusions can be summarized in the following way.

- (1) The opening force variation was numerically evaluated by using the derived formula including the maximum value. The experimental measurement shows that the error is within 13%.
- (2) The effect of the rail curvature on the opening force was clarified as well as the effect of the height of the rotation fulcrum at the end of the guide rail. By using a torsion spring in the rotation fulcrum A, the opening force can be less than the target value of 19.6 N.

- (3) To obtain the enough passage width for wheelchairs, the horizontal dimension of the storage space was set as small as possible (see Figure 11(a)). The guide rail with the circular arc radius $R = 478$ mm is set to reduce the maximum opening force. The relative positions between the rotation fulcrum A and the guide roller B are determined to realize the smooth movement of the handrail when the guide rail geometry was determined.
- (4) The guide rail geometry consists of three straight line and three circular arc sections. The straight line 1 and the circular arc 1 may allow the position error when the door is installed to close the door completely. The circular arc 2 and the straight line 2 are set to produce the initial opening force $F_{Ax}(x_A) = 5$ N in Figure 10(a). This is because a small initial opening force $F_{Ax}(x_A) < 5$ N is dangerous for elderly people. The handrail is gently bent to avoid interference between the handle and the handrail when the sliding door is fully opened (see the red circle in Figure 11(a)).
- (5) To secure the safety of the sliding door, a repeated opening/closing test was conducted. The results show that the retractable handrail and the sliding door may withstand 200,000 cycles within an increase of the running resistance by about 10% due to wear appearing on the built-in wheels and the sliding door rail surface.

References

- [1] Ando, T. (1968). Rolling friction, Mechanical Engineers' Handbook (5th ed.). The Japan Society of Mechanical Engineers.
- [2] Arfken, C. L., Lach, H. W., Birge, S. J., & Miller, J. P. (1994). The prevalence and correlates of fear of falling in elderly persons living in the community. *Am J Public Health*, 84, 565-570. DOI: [10.2105/ajph.84.4.565](https://doi.org/10.2105/ajph.84.4.565)
- [3] Chihara, T. & Seo, A. (2014). Evaluation of multiple muscle loads through multi-objective optimization with prediction of subjective satisfaction level: Illustration by an application to handrail position for standing. *Applied Ergonomics*, 45(2), 261-269. DOI: [10.1016/j.apergo.2013.04.006](https://doi.org/10.1016/j.apergo.2013.04.006)

- [4] Chu, L. W., Pei, C. K. W., Chiu, A., Liu, K., Chu, M. M., Wong, S., & Wong, A. (1999). Risk factors for falls in hospitalized older medical patients. *Journal of Gerontology: Series A*, 54(1), M38-M43. DOI: [10.1093/gerona/54.1.m38](https://doi.org/10.1093/gerona/54.1.m38)
- [5] Cumming, G. R., Salkeld, G., Thomas, M., & Szonyi, G. (2000). Prospective study of the impact of fear of falling on activities of daily living, SF-36 scores, and nursing home admission. *Journal of Gerontology: Series A*, 55(5), M299-M305. DOI: [10.1093/gerona/55.5.m299](https://doi.org/10.1093/gerona/55.5.m299)
- [6] Dusenberry, D. O., Simoson, H., DelloRusso, S. J., & Rao, R. S. (2009). Effect of handrail shape on graspability. *Applied Ergonomics*, 40(4), 657-669. DOI: [10.1016/j.apergo.2008.05.006](https://doi.org/10.1016/j.apergo.2008.05.006)
- [7] Gault, M. L., & Willems, M. E. (2013). Aging, functional capacity and eccentric exercise training. *Aging and Disease*, 4(6), 351-363. DOI: [10.14336/AD.2013.0400351](https://doi.org/10.14336/AD.2013.0400351)
- [8] Gunter, K. B., White, K. N., Hayes, W. C., & Snow, C. M. (2000). Functional Mobility discriminates nonfallers from one-time and frequent fallers. *Journal of Gerontology: Series A*, 55(11), M672-M676. DOI: [10.1093/gerona/55.11.M672](https://doi.org/10.1093/gerona/55.11.M672)
- [9] Howland, J., Lachman, M. E., Peterson, E. W., Cote, J., Kasten, L., & Jette, A. (1998). Covariates of fear of falling and associated activity curtailment. *The Gerontologist*, 38(5), 549-555. DOI: [10.1093/geront/38.5.549](https://doi.org/10.1093/geront/38.5.549)
- [10] Ishihara, K., Nagamachi, M., Komatsu, K., Ishihara, S., Ichitsubo, M., Mikami, Y., Osuga, Y., Imamura, K., & Osaki, H. (2002). Handrails for the elderly: A survey of the need for handrails and experiments to determine the optimal size of staircase handrails. *Gerontechnology*, 1(3), 175-189. DOI: [10.4017/gt.2001.01.03.006.00](https://doi.org/10.4017/gt.2001.01.03.006.00)
- [11] Itoh, T. (2007). Sliding door for passenger conveyor (Patent No. 4012869). Japan Patent Office. <https://www.j-platpat.inpit.go.jp/>
- [12] Kim, H., Yoshida, H., & Suzuki, T. (2001). Fall-related fear and physical function in the elderly: About fall outpatients. *Japan Geriatrics Society*, 38(6), 805-811. DOI: [10.3143/geriatrics.38.805](https://doi.org/10.3143/geriatrics.38.805)
- [13] Kitamura, A. (2007). The extensible prop-up type post. (Patent application No. 3952370). Japan Patent Office. <https://www.j-platpat.inpit.go.jp/>
- [14] Kubo, Y. (2011). The sliding door, the handrail for the sliding door device. (Patent No. 4639358). Japan Patent Office. <https://www.j-platpat.inpit.go.jp/>

- [15] Kubo, Y. (2017). The sliding door, the handrail for the sliding door device. (Patent No. 6174304). Japan Patent Office. <https://www.j-platpat.inpit.go.jp/>
- [16] Lachman, M. E., Howland, J., Tennstedt, S., Jette, A., Assmann, S., & Peterson, E. W. (1998). Fear of falling and activity restriction: The survey of activities and fear of falling in the elderly. *Journal of Gerontology: Series B*, 55B(1), 43-50. DOI: [10.1093/geronb/53b.1.p43](https://doi.org/10.1093/geronb/53b.1.p43)
- [17] Mazroc Co., Ltd. (2019). Flip-up type handrail. Retrieved November 6, 2020, from https://www.mazroc.co.jp/products_1/series/1007/CB_01
- [18] Min, N. S., Kim, J. Y., & Parnianpour, M. (2012). The effects of safety handrails and the heights of scaffolds on the subjective and objective evaluation of postural stability and cardiovascular stress in novice and expert construction workers. *Applied Ergonomics*, 43(3), 574-581. DOI: [10.1016/j.apergo.2011.09.002](https://doi.org/10.1016/j.apergo.2011.09.002)
- [19] Porter, M. M., Vandervoort, A. A., & Lexell, J. (1995). Aging of human muscle: structure, function and adaptability. *Scandinavian Journal of Medicine & Science in Sports*, 5(3), 129-142. DOI: [10.1111/j.1600-0838.1995.tb00026.x](https://doi.org/10.1111/j.1600-0838.1995.tb00026.x)
- [20] Sasuga, I. (2003). Fatigue life of torsion coil spring: Application of fatigue limit diagram. *Machine Design*, 47(11), 130-134.
- [21] Tanaka, S., Akazawa, K., Nunota, K., Satoh, K., Katoh, M., Gotoh, Y., Yokobayashi, Y., & Kose, S. (2004). Relationship between applied force and the shape and dimensions of the operating part of sliding doors considering use by elderly people. *Transactions of Japanese Society for Medical and Biological Engineering*, 42(4), 347-353. DOI: [10.11239/jsmbe2002.42.347](https://doi.org/10.11239/jsmbe2002.42.347)
- [22] World Health Organization. (2007). WHO global report on falls prevention in older age [PDF file]. Retrieved from https://www.who.int/ageing/publications/Falls_prevention7March.pdf

How to cite this article:

Saitou, K. & Noda, N. (2021). Semi-automatic retractable handrail utilizing opening/closing movement of sliding door supporting elderly people to walk independently. *Accessibility and Design for All*, 11(1), 1-19.
<https://doi.org/10.17411/jacces.v11i1.327>

The [Journal of Accessibility and Design for All](#), ISSN 2013-7087, is published by the [Universitat Politècnica de Catalunya, Barcelona Tech](#) with the sponsoring of [Fundación ONCE](#). This issue is free of charge and is available in electronic format.

This work is licensed under an **Attribution-Non Commercial 4.0 International Creative Commons License**. Readers are allowed to read, download, copy, redistribute, print, search, or link to the full texts of the articles, or use them for any other lawful purpose, giving appropriated credit. It must not be used for commercial purposes. To see the complete license contents, please visit <http://creativecommons.org/licenses/by-nc/4.0/>.

JACCES is committed to providing accessible publication to all, regardless of technology or ability. Present document grants strong accessibility since it applies to WCAG 2.0 and accessible PDF recommendations. Evaluation tool used has been Adobe Acrobat® Accessibility Checker. If you encounter problems accessing content of this document, you can contact us at jacces@catac.upc.edu.